Biophysical Journal Volume 73 July 1997 348–356

Supramolecular Self-Assembly of $d(TGG)_4$, Synergistic Effects of K^+ and Mg^{2+}

Fu-Ming Chen
Department of Chemistry, Tennessee State University, Nashville, Tennessee 37209-1561 USA

ABSTRACT Spectral evidence indicates that molar concentrations of K^+ can induce aggregate formation in $d(TGG)_4$. The 320-nm turbidity monitoring indicates that more than 1 M KCl is needed for the onset of aggregation to occur at 20°C within the time span of 24 h. The kinetic profile is reminiscent of autocatalytic reactions that consist of a lag period followed by accelerative and leveling phases. Progressive shortening of lag periods and more rapid accelerative phases accompany further increases in $[K^+]$. Interestingly, the presence of Mg^{2+} greatly facilitates the aggregate formation and results in the prominent appearance of an intense ψ-type CD. For example, whereas 1 M K^+ fails to induce aggregate formation of $d(TGG)_4$ within 24 h, the addition of 1 mM Mg^{2+} to a 1 M K^+ solution is sufficient to induce the onset of aggregation in approximately 12 h. Furthermore, adjustment of the buffer to 16 mM Mg^{2+}/1 M KCl reduces the lag time to less than 10 min and aggregation is nearly complete in 2 h. The requirement of $[K^+]$ for aggregation is reduced to 2 mM in the presence of 16 mM Mg^{2+}, a reduction of nearly three orders of magnitude when compared to solutions without Mg^{2+}. The effects of K^+ and Mg^{2+} ions are synergistic, because the presence of 16 mM Mg^{2+} alone does not induce aggregate formation in this oligomer. Thermal stabilities of the aggregates are strongly dependent on the concentrations of these two ions. Although aggregates formed in the presence of 2 M KCl alone melt around 55°C, those formed with added 16 mM Mg^{2+} melt at ~90°C, with some aggregates remaining unmelted even at 95°C. The slow kinetics of aggregate formation led to the appearance of gross hystereses in the cooling profiles. The interplay of these two ions appears to be specific, because the replacement of K^+ by Na^+ or the replacement of Mg^{2+} by other divalent cations does not lead to the observed self-assembly phenomeon, although Sr^{2+} can substitute for K^+. A possible mechanism for the formation of self-assembled structures is suggested.

INTRODUCTION

Our laboratory has recently uncovered a rather interesting phenomenon in which molar $[K^+]$ induces aggregate formation of $d(CGG)_4$, as indicated by 1) intense ψ-type circular dichroic (CD) spectra (a huge CD band with long-wavelength tail), 2) the presence of absorbance tails at wavelengths well above 310 nm, and 3) the appearance of high-molecular-weight species on electrophoretic gels (Chen, 1995). The rates of aggregation are extremely slow at pH 8 but are greatly enhanced in acidic conditions. The kinetic profiles resemble those of autocatalytic reacting systems, showing characteristic lag periods followed by accelerative phases. Time-dependent CD spectral characteristics indicate an initial positive intensity enhancement near 265 nm, suggesting the formation of parallel G-tetraplexes before the onset of aggregation. Both $d(TGG)_4$ and $d(CGG)_4T$ fail to exhibit the induction of ψ-CD spectra under similar conditions, suggesting that the terminal G and the base protonation of cytosine play crucial roles in the observed phenomenon. Finally, the aggregations are not induced by molar concentrations of NaCl. To explain these observations, we proposed that parallel quadruplexes may form initially and be converted to quadruplexes with contiguous G-tetrads and looped-out cytosines in the presence of high $[K^+]$. These quadruplexes could stack vertically and expand horizontally via interquadruplex C^+·C base pairing to result in dendrimer-type self-assembled superstructures.

We report here the results of a more detailed study with $d(TGG)_4$ that reveals this oligomer can also be induced to form aggregates under appropriate conditions. Absorbance (turbidity) data indicate that this oligomer forms aggregates in the presence of molar K^+. The presence of Mg^{2+} greatly facilitates aggregation and leads to the formation of large Ψ-CD spectra. The effects of K^+ and Mg^{2+} on the aggregation of this oligomer appear to be synergistic.

MATERIALS AND METHODS

Synthetic oligonucleotides were purchased from Research Genetics (Huntsville, AL) and used without further purification. These oligomers were purified by the vendor via reverse-phase oligonucleotide purification cartridges and exhibited single-band electrophoretic mobilities in denaturing polyacrylamide gel electrophoresis with stated purities of ≥95%. Concentrations of oligomers (per nucleotide) were determined by measuring absorbances at 260 nm after melting, with the use of extinction coefficients obtained via nearest-neighbor approximation using mono- and dinucleotide values tabulated in Fasman (1975). Aggregation kinetic profiles were obtained by maintaining the temperature at 20°C and monitoring the time-dependent absorbance changes at 320 nm. The reaction was initiated by addition of the appropriate amount of oligomeric stock to a buffer solution containing the desired salt concentrations. Thermal denaturation experiments were carried out with 1-cm semimicro cells by monitoring absorbances at appropriate wavelengths. A heating (or cooling) rate of 0.5°C/min was maintained by the temperature controller accessory. CD spectra were measured with a Jasco J-500A recording spectropolarimeter using water-jacketed cylindrical cells of 1 cm path length. All experiments

Received for publication 21 January 1997 and in final form 24 March 1997.

Address reprint requests to Dr. Fu-Ming Chen, Department of Chemistry, Tennessee State University, Nashville, TN 37209-1561. Tel.: 615-963-5325; Fax: 615-963-5434; E-mail: chenf@harpo.tnstate.edu.

0006-3495/97/07/348/09 $2.00

were carried out in 10 mM HEPPS (*N*-(2-hydroxyethyl)-piperazine-*N'*-propanesulfonic acid) buffer solutions of pH 8 (adjusted by droplet additions of 1 M NaOH). In contrast to our work on $d(CGG)_4$, no 0.1 M NaCl was added to the buffer.

RESULTS

Absorbance monitoring of K^+-induced aggregate formation in $d(TGG)_4$

Ordinary DNA exhibits an absorbance maximum near 260 nm and is transparent to light beyond 310 nm. Absorbance at the long wavelengths, however, can be induced by the solution turbidity due to the presence of aggregated particulates. The absorbance evidence on the K^+-induced aggregation of $d(TGG)_4$ is shown in Fig. 1 *A*, where the kinetic profiles via 320-nm monitoring are presented for solutions containing molar amounts of KCl. It is apparent that the kinetics of aggregation are autocatalytic-like, with a characteristic lag period being followed by an accelerative phase of absorbance increase and an eventual leveling. Only a hint of absorbance increase is evident near 650 min in the presence of 1.2 M KCl, and equilibrium was not reached until several days later. In contrast, the onset of aggregation can more clearly be discerned near 300 min in the 1.4 M KCl solution. The progressive shortening of the lag periods, along with the appearance of more rapid accelerative phases, is apparent with further increases in $[K^+]$. In a 2.6 M KCl solution, for example, a lag period of less than 10 min is seen, and the aggregation is nearly complete in about 2 h. The decreases in absorbance, evident at longer times for solutions containing higher $[K^+]$, most likely are the consequence of slow sedimentations of larger aggregated particles, inasmuch as rigorous shaking of the cuvettes after the run results in significantly higher absorbance readings.

Mg^{2+} greatly facilitates the K^+-induced aggregate formation

The presence of Mg^{2+} in solutions greatly facilitates the K^+-induced aggregate formation of $d(TGG)_4$. The intricate interplay of these two cations is illustrated by the effects of Mg^{2+} on the kinetic profiles of the 1 M KCl-induced aggregate formation of 40 μM $d(TGG)_4$ (Fig. 1 *B*). Although no sign of aggregate formation is detected in a time span of 24 h (1440 min) for a 1.0 M KCl solution (not shown), the mere presence of 1 mM Mg^{2+} leads to the appearance of an absorbance increase starting around 750 min. A dramatic reduction in the lag period and the concomitant appearance of a more rapid accelerative phase are evident as the $[Mg^{2+}]$ is progressively increased. For example, the presence of 8 mM Mg^{2+} reduces the lag period to ~1 h, similar to that of 2.0 M KCl solution without divalent cation (see Fig. 1 *A*), but with a much steeper accelerative phase. Furthermore, the presence of 16 mM Mg^{2+} reduces the lag time to less than 10 min, and the reaction appears to be nearly complete in ~2 h.

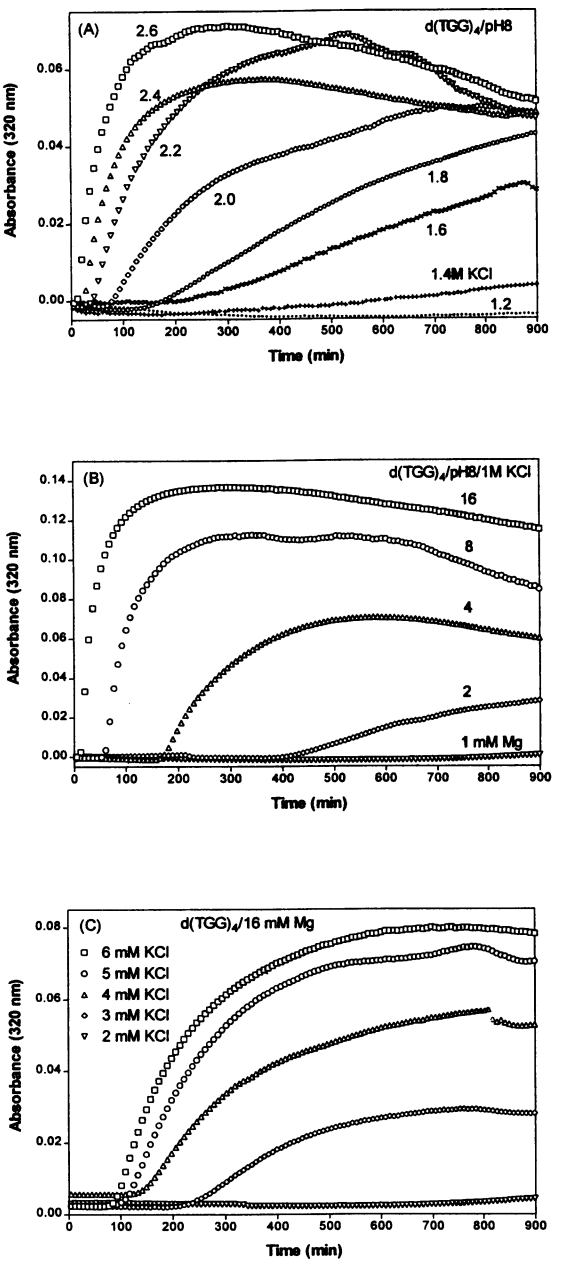

FIGURE 1 Aggregation kinetic profiles of 40 μM (in nucleotide) $d(TGG)_4$ at pH 8 via 320-nm absorbance monitoring at 20°C. (*A*) Comparison of solutions in the presence of different $[K^+]$ with no Mg^{2+}. (*B*) Comparison of solutions in the presence of 1 M KCl and differing $[Mg^{2+}]$. (*C*) Comparison of solutions containing 16 mM Mg^{2+} and differing $[K^+]$. Reactions were initiated by adding the appropriate amounts of DNA stocks with the use of a stirrer accessory into pH 8 solutions containing the desired cation concentrations.

Synergistic effects of K^+ and Mg^{2+} in aggregate formation

The effect of Mg^{2+} in lowering the requirement of KCl for aggregation of oligomers can be seen by comparing the kinetic profiles of 40 μM $d(TGG)_4$ in the presence of 16 mM Mg^{2+} and differing amounts of KCl (Fig. 1 *C*). It is apparent that 2 mM KCl is sufficient to induce the aggregate

formation of $d(TGG)_4$ in a 16 mM Mg^{2+} solution (as indicated by the onset of absorbance enhancement near 700 min), whereas 1.2 M KCl is needed to produce this effect in the absence of Mg^{2+} (see Fig. 1 *A*), reflecting a reduction of nearly three orders of magnitude in the K^+ requirement. Additional 1.5- and 2-fold increases in $[K^+]$ (from 2 mM to 3 and 4 mM, respectively) lead to decreases in the lag times to 240 and 120 min, respectively. Furthermore, even though the onset of aggregation for 40 μM $d(TGG)_4$ in the presence of 16 mM Mg^{2+} and 6 mM K^+ occurs at roughly the same time (70–80 min) as that of 2 M KCl alone, a more rapid accelerative phase is clearly evident. The further shortening of lag periods and more rapid accelerative phases for aggregate formation are seen with further increases in KCl concentrations (not shown). The synergistic effect of these two cations is shown by the inability of 16 mM Mg^{2+} to cause aggregate formation in the absence of K^+.

Melting profiles of the aggregates and the gross cooling hystereses

Thermal stabilities of aggregates can be revealed by the melting profiles obtained from monitoring the absorbance decrease at 320 nm as complexes are denatured. Melting profiles of aggregates formed in the presence of differing amounts of KCl alone are shown in Fig. 2 *A*. As expected, the melting temperature increases as the $[K^+]$ is increased and the melting profiles become progressively more cooperative. In contrast to most regular duplex DNA melting, the cooling profiles of these solutions are seen to exhibit gross hystereses, as exemplified in solutions containing 2.8 and 2.4 M KCl. Although the melting temperatures for the 2.8 and 2.4 M KCl-induced aggregates are close to 65°C and 61°C, respectively (see Fig. 1 *A*), their cooling profiles provide no sign of reaggregation (as indicated by the 320-nm absorbance increase) until around 55°C and 40°C, respectively, with only ~15% and <10% recoveries by the time they reach 20°C. It may be of interest to note that, although the melting temperature of the aggregates is progressively increased as $[K^+]$ is inceased, the 320-nm absorbance exhibits an unexpected progressive decrease as the $[K^+]$ exceeds 2.6 M (compare the 2.6 and 2.8 M KCl profiles). This may be a consequence of changes in the nature of aggregates formed at higher ionic strengths, such as the formation of smaller particles.

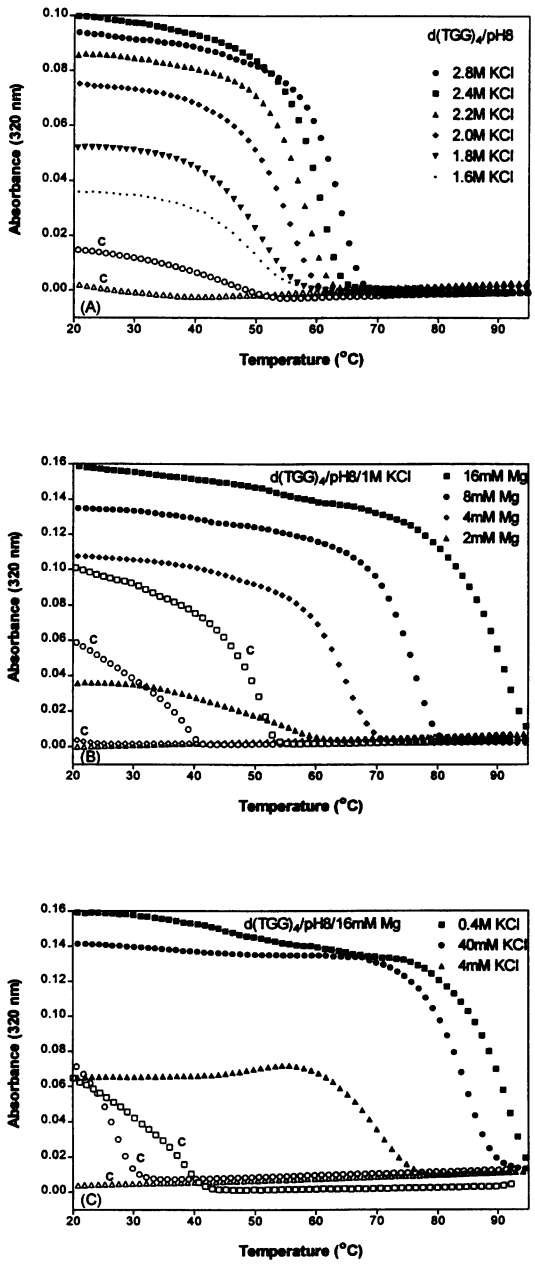

FIGURE 2 Melting profiles of $d(TGG)_4$ aggregates formed by 40 μM nucleotide at pH 8 under various ionic conditions. Corresponding open symbols are those of cooling profiles (with c designations). (*A*) Comparison of melting profiles of aggregates formed by molar KCl in the absence of Mg^{2+}. (*B*) Comparison of melting profiles of aggregates formed by 1.0 M KCl in the presence of differing $[Mg^{2+}]$. (*C*) Representative melting profiles of aggregates formed by differing $[K^+]$ in the presence of 16 mM Mg^{2+}.

Thermal stabilities of aggregates are greatly enhanced by the presence of Mg^{2+}

The effects of Mg^{2+} on the thermal stabilities of the aggregates can be seen by a comparison of melting profiles of aggregates formed by 1 M KCl and in the presence of differing $[Mg^{2+}]$, as shown in Fig. 2 *B*. It is apparent that the presence of Mg^{2+} dramatically enhances the thermal stabilities of the aggregates. For example, the 1 M KCl-induced aggregates melt around 50°C in the presence of 2 mM Mg^{2+}; further two-, four-, and eightfold increases in $[Mg^{2+}]$ result in melting temperatures of 65°C, 75°C, and 89°C, respectively. In fact, a small fraction of aggregates in the latter solution were not completely melted at 95°C, as evidenced by the residual 320-nm absorbance retained at this temperature. Representative cooling profiles are included to highlight the gross hysteretic effects. For example,

there is no hint of reaggregation of oligomer in solutions containing 2 mM Mg^{2+}, even when returning to 20°C. The onset of reaggregation for solutions containing 4, 8, and 16 mM Mg^{2+} is evident near 25°C, 41°C, and 53°C, respectively.

The effect of K^+ on the thermal stability of aggregates formed by $d(TGG)_4$ in solutions containing 16 mM Mg^{2+} is shown in Fig. 2 *C*. As can be seen, a 10-fold increase in $[K^+]$ from 4 to 40 mM increases the melting temperature from 68°C to 84°C, and an additional 10-fold increase from 40 to 400 mM increases it to ~90°C. The cooling profiles again exhibit gross hystereses, with the onset of reaggregation occurring near 43°C and 34°C, respectively, in solutions containing 400 and 40 mM K^+, and showing no sign of reaggregation upon returning to 20°C in solutions containing 4 mM K^+.

ψ-CD spectral characteristics

A highly condensed form of DNA is sometimes characterized by a CD spectrum an order of magnitude higher in intensity than that of unaggregated DNA (Shin and Eichhorn, 1984). This so-called ψ-type CD is presumably a manifestation of differential light scattering and superorganization of the DNA in the aggregates (Maestre and Reich, 1980). Consequently, ψ-CD spectral characterization of the aggregates formed will be of interest.

Time-dependent CD spectral characteristics under various solution conditions are compared in Fig. 3. Spectral alterations in a solution containing 2.0 M KCl are shown in Fig. 3 *A*. The oligomer initially exhibits a spectrum with a weak positive CD maximum near 265 nm. The onset of spectral intensity enhancement commences after a latent lag period of ~50 min to eventually develop into a spectrum consisting of a positive maximum at 265 nm with a shoulder near 290 nm and a negative long-wavelength tail. Except for a much shorter lag period of less than 10 min and a more dramatic intensity enhancement, the spectral features of the 2.8 M KCl solution (Fig. 3 *B*; note the fourfold vertical scale increase) are not very different. Spectral features in solutions containing 16 mM Mg^{2+} and two different $[K^+]$ are shown in Fig. 3, *C* and *D*, respectively. The presence of Mg^{2+} enhanced the absorbance near 290 nm relative to that near 265 nm, producing a positive maximum at 290 nm, a shoulder near 265 nm, and a positive (0.01 M KCl, Fig. 3 *C*) or a weak negative (1.0 M KCl, Fig. 3 *D*) long-wavelength tail.

CD spectral measurements were also made after melting the aggregates and cooling the solutions back to room temperature and waiting for a few days. Interestingly, the postmelt spectra were strongly dependent on solution conditions. For example, a further intensity enhancement with a slight red-shift as compared to the premelt spectrum is seen for the solution containing 16 mM Mg^{2+} and 1.0 M KCl (note the 1.5-fold reduction in intensity for the solid curve to fit into the scale of Fig. 3 *D*). In contrast, a much weaker bisignate CD with negative and positive maxima near 300 and 265 nm, respectively, developed in the 2.8 M KCl solution (see the *solid curve* of Fig. 3 *B*).

The kinetics of spectral alterations can be seen more clearly by monitoring ellipticity changes at individual wavelengths, as shown in Fig. 4. Consistent with those of absorbance monitoring, the kinetics are autocatalytic-like, exhibiting a lag period and an accelerative phase. A dramatic reduction in the lag period from ~50 to less than 10 min and a more rapid accelerative phase are seen when $[K^+]$ increases from 2.0 to 2.8 M (compare Fig. 4, *A* and *B*). The facilitation of ψ-CD by Mg^{2+} is illustrated by the less than 10 min lag time needed for aggregate formation in the presence of 16 mM Mg^{2+}/1.0 M KCl (see Fig. 4 *D*). No onset of aggregation is evident in the time span of 1440 min (24 h) in the absence of the divalent cation. Furthermore, 16 mM Mg^{2+} alone does not induce spectral alterations, but the presence of 10 mM KCl leads to aggregate formation with a lag time of slightly over 1 h (see Fig. 4 *C*). The development of a large positive CD tail is indicated by the sizable positive-going kinetic profile of the 310-nm ellipticity monitoring of this solution.

Other divalent cations failed to exhibit similar effects

To determine whether divalent cations other than Mg^{2+} affect the aggregation of $d(TGG)_4$, rudimentary studies were made with Sr^{2+}, Ba^{2+}, Zn^{2+}, and Ni^{2+}. The results indicate these ions are not effective in promoting aggregate formation by the oligomer in solutions with K^+. Interestingly, however, our preliminary results suggest some synergistic effect between Sr^{2+} and Mg^{2+}, similar to that exhibited by K^+ and Mg^{2+}.

DISCUSSION

Our results indicate that molar K^+ induces aggregate formation by $d(TGG)_4$. In fact, the onset of aggregation occurs near 1 h at 20°C at pH 8 in the presence of 2 M KCl. This is considerably faster than that of $d(CGG)_4$ under similar conditions (Chen, 1995). The features of the kinetic profiles are like those of autocatalytic reactions, consisting of a lag period followed by accelerative and leveling phases. Interestingly, the presence of Mg^{2+} greatly enhances aggregate formation and results in the prominent appearance of an intense ψ-type CD spectrum. In contrast to the absence of aggregate formation in a time span of 24 h (1440 min) in a 1 M K^+ solution at 20°C, the presence of 1 mM Mg^{2+} induces aggregate formation in ~700 min, and 16 mM Mg^{2+} induces aggregation in less than 10 min. Furthermore, the presence of 16 mM Mg^{2+} reduces the requirement for K^+ on aggregation to merely 2 mM. The effects of K^+ and Mg^{2+} ions appear to be synergistic, inasmuch as the presence of 16 mM Mg^{2+} alone does not induce aggregate formation in this oligomer. In addition, thermal stabilities of the aggregates are strongly dependent on the concentrations

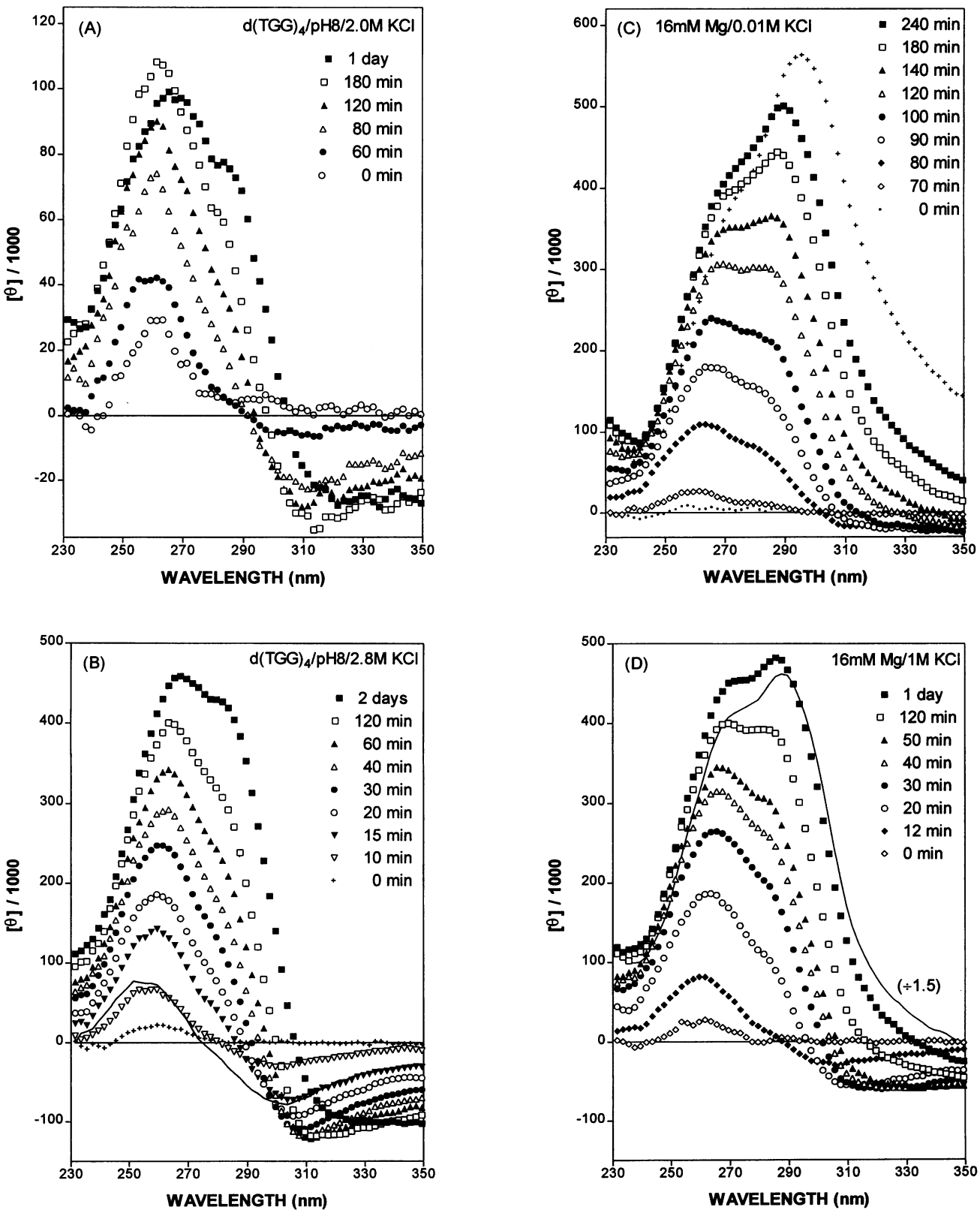

FIGURE 3 Comparison of time-dependent CD spectra for 40 μM d(TGG)$_4$ at pH 8 under various solution conditions. (*A*) In the the presence of 2.0 M KCl. (*B*) In the presence of 2.8 M KCl. The solid curve is that of the postmelt spectrum after a few days. (*C*) In the presence of 16 mM $MgCl_2$ and 0.01 M KCl. The (+) curve is the spectrum after a few days. (*D*) In the presence of 16 mM $MgCl_2$ and 1.0 M KCl. The solid curve is that of postmelt spectrum after a few days (with 1.5-fold reduction in intensity to fit into the scale).

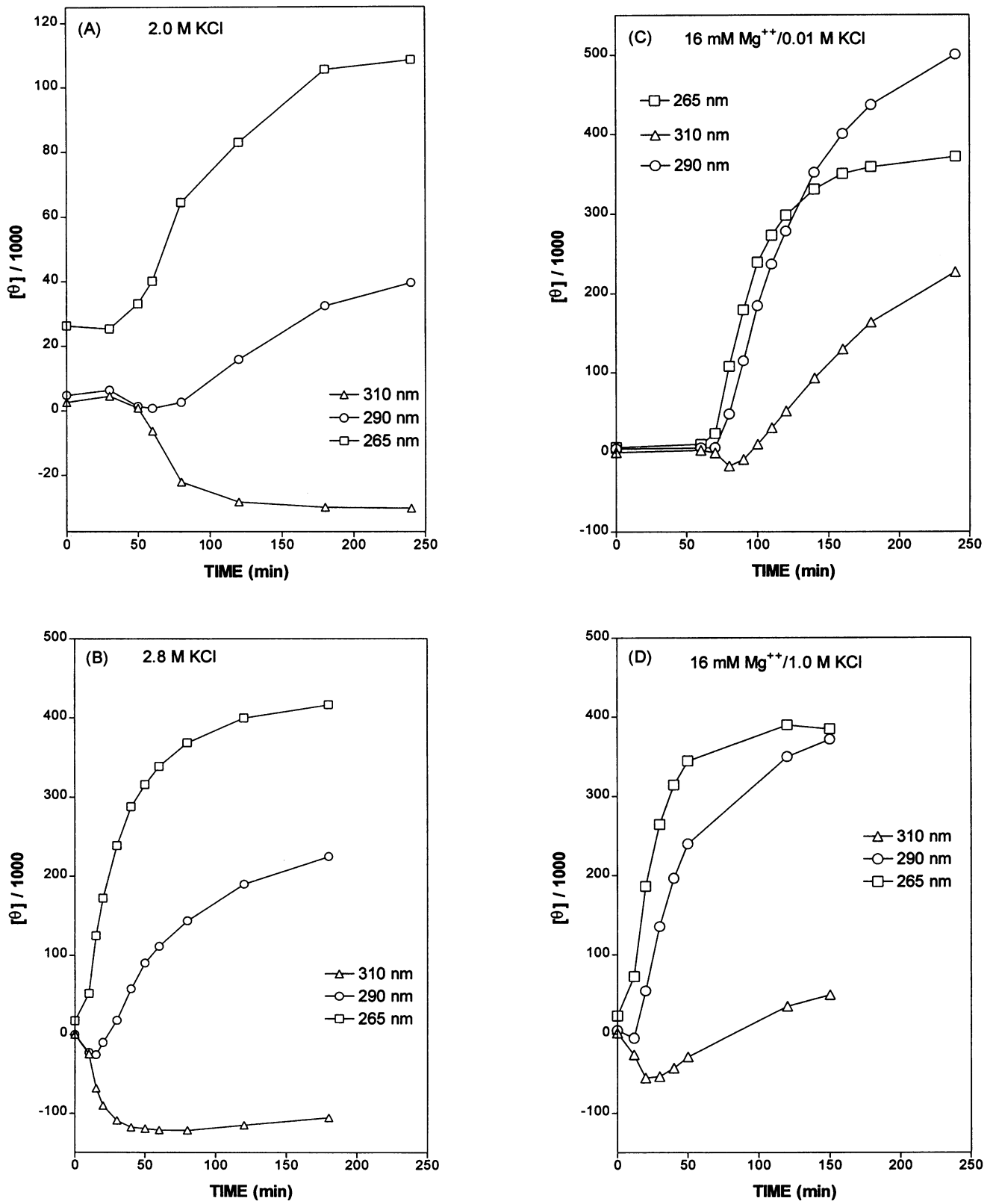

FIGURE 4 Comparison of aggregation kinetic profiles at 20°C via ellipticity monitoring at 310, 290, and 265 nm for 40 μM d(TGG)$_4$ under various solution conditions. (*A*) In the presence of 2.0 M KCl. (*B*) In the presence of 2.8 M KCl. (*C*) In the presence of 16 mM $MgCl_2$ and 0.01 M KCl. (*D*) In the presence of 16 mM $MgCl_2$ and 1.0 M KCl.

of these two ions, and their cooling profiles exhibit gross hystereses. Although the aggregates formed by 2 M KCl alone melt around 55°C, the presence of 16 mM Mg^{2+} increases the melting temperature to ~90°C, with some aggregates remaining unmelted even at 95°C. The interplay of these two ions in the aggregation process appears to be specific, because the replacement of K^+ by Na^+ or the replacement of Mg^{2+} by other divalent cations does not appear to lead to the observed self-assembly phenomenon. However, synergistic effects have been observed with Sr^{2+} and Mg^{2+}.

The observed synergism exhibited by K^+ and Mg^{2+} is consistent with reports by Dai et al. (1995) and Marotta et al. (1996) that oligomers of the form $C_4T_4G_4T_{1-4}G_4$ and $G_xT_2G_y$ self-assemble into multistranded species of high molecular weight in the presence of 100 mM K^+ plus 20 mM Mg^{2+}, but not in the presence of 100 mM K^+, 20 mM Mg^{2+}, or 100 mM Na^+ alone. In contrast to our observations on $d(CGG)_4$ and $d(TGG)_4$, however, their systems do not appear to exhibit ψ-CD spectral characteristics.

In view of the facilitation of this process by the divalent cation Mg^{2+}, it is possible the oligomer forms parallel-stranded homoduplexes in solutions that (aided by the higher concentration and optimal size of K^+ that fits into quadruplex cages) subsequently form in- and/or out-of-register quadruplexes (see Fig. 5). Axial extension of the out-of-register quadruplexes could result if repeated quadruplex formation occurred with sticky ends forming G-wires (Marsh and Henderson, 1994; Dai et al., 1995), whereas those of in-register quadruplexes could result from vertical head-to-tail stacking. In addition, lateral expansion may be achieved by interquadruplex associations via phosphate-Mg^{2+} bond formation. The role of Mg^{2+} in the self-assembly process may be 1) to facilitate the initial homoduplex and subsequent tetraplex formation for axial extension via phosphate charge neutralization and 2) to bridge interquadruplex phosphate groups for lateral expansion, as a consequence of the strong affinity of this divalent cation for phosphates.

The speculated stepwise formation of the self-assembled structure is consistent with the observations of autocatalytic-type kinetics, because each product provides further reaction sites analogous to the products of chain branching polymerization, and with observations of the gross hystereses exhibited by the melting profiles of the aggregates, a consequence of the slow formation kinetics of the aggregates.

The notion of the initial formation of parallel-stranded homoduplexes appears to be supported by a recent study of Suda et al. (1995) on oligonucleotides consisting of a double-helical stretch followed by a single-stranded 3′-terminal overhang of nine GGA sequence repeats. Clever gel electrophoretic experiments led to the conclusion that the $d(GGA)_9$ segment dimerizes in a parallel orientation via G·G base pairings. It was also noted that the parallel homoduplex formation of some of their oligomers and oligonucleotides containing d(GA) repeats (Rippe et al., 1992) was

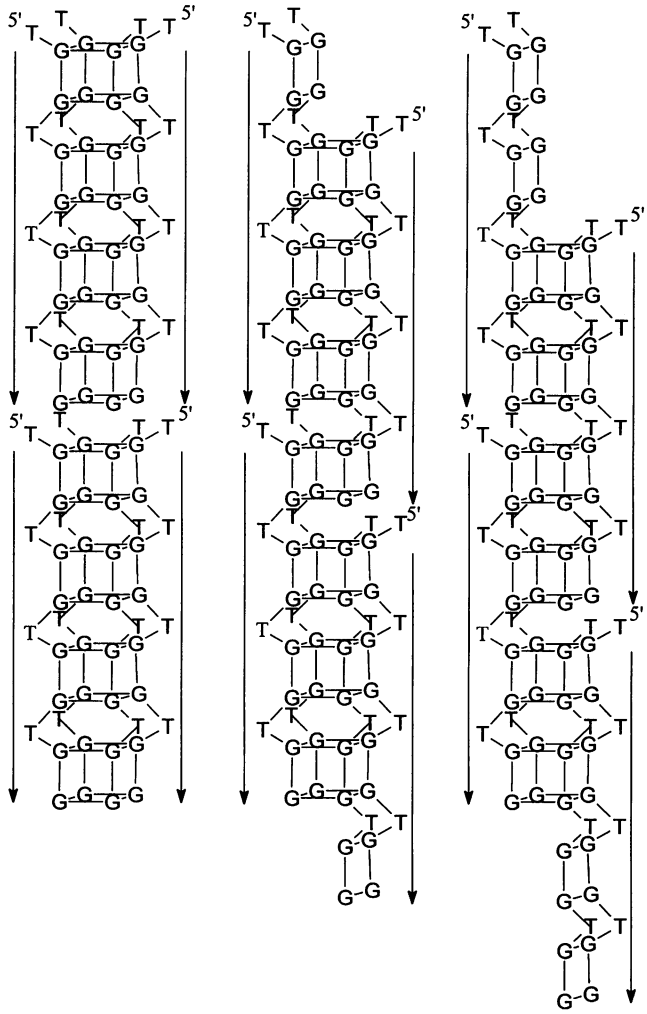

FIGURE 5 Schematic drawings of some possible means of axial extension via in- and out-of-register K^+-driven quadruplex formation (the indicated contiguous G-quartets and looped-out thymidines are purely speculative). For simplicity, only eight strands of $d(TGG)_4$ are shown in the illustration. Lateral expansion via Mg^{2+}-mediated interquadruplex associations (through P-Mg^{2+}-P interactions) is not shown. K^+ ions sandwiched between each pair of G-tetrads are also not shown.

greatly facilitated by Mg^{2+}. Thus considerable ease in aggregate formation should be expected for the AGG trinucleotide repeats, as is indeed borne out by our preliminary studies with $d(AGG)_4$.

The suggested formation of parallel G-quadruplexes before the onset of aggregation is supported by the initial appearance of a characteristic positive 265-nm CD maximum (Balagurumoorthy et al., 1992; Chen, 1992; Hardin et al., 1991) and an earlier observation of Lee (1990) indicating the formation of parallel tetraplex in polyd(GGA). The requirement of molar K^+ for the assembly of $d(CGG)_4$ and $d(TGG)_4$ oligomers and the failure of Na^+ to induce a similar phenomenon under the same conditions also supports the mechanism of initial quadruplex formation of parallel orientation. It is known that Na^+ is too small, but K^+ is the right size for forming a stable octa-coordinated

complex with two G-quartets. Recent Raman studies by Miura et al. (1995) on the quadruplex formation of d(TTTTGGGG)$_4$ further led to the finding that both Na^+ and K^+ facilitate an antiparallel foldback quadruplex at low concentrations but a parallel quadruplex at higher concentrations, with K^+ being more effective in inducing the parallel association. The need for K^+ and a terminal G in the formation of higher ordered structures had been reported by Sen and Gilbert (1992) and Lu et al. (1992). Sen and Gilbert (1992) have shown that oligomers containing a single multiguanine motif at their 3′ or 5′ end, with a guanine as the terminal base, can form higher order products. Methylation protection experiments suggest a nested head-to-tail superstructure containing tetraplexes bonded front-to-back via G quartets formed by out-of-register guanines.

Our speculated mechnism is consistent with the finding that at pH 8, $d(TGG)_4$ aggregates more readily than $d(CGG)_4$ under the same conditions. In contrast, aggregation of $d(CGG)_4$ is facilitated by acidic conditions (Chen, 1995). The presence of cytosines in $d(CGG)_4$ may have trapped this oligomer in conformations that utilize G · C base pairings, such as dimeric duplex or monomeric hairpins, so as to reduce the existence of single-stranded conformers for ease of quadruplex formation. Thus our earlier observed acid-facilitation of aggregate formation in $d(CGG)_4$ may partly be the consequence of the destabilization of these trapped conformers resulting from weakened G · C base pairs due to base protonation of cytidine, and partly the consequence of the facilitation of parallel duplex and/or quadruplex formation via C · C^+ base pairings (Hardin et al., 1992, 1993).

We suggest that synergistic effects of K^+ and Mg^{2+} are the consequence of complementary roles played by these two cations, the ability to facilitate the parallel quadruplex formation by the former and binding of phosphate by the latter. The inability of Mg^{2+} to induce aggregation in the absence of K^+ supports the important role of parallel quadruplex formation in the supramolecular self-assembly in $d(TGG)_4$. Thus our rudimentary observation of the ability of Sr^{2+} to synergistically affect aggregation with Mg^{2+} is consistent with the fact that Sr^{2+} has also been shown to facilitate parallel quadruplex formation (Chantot and Guschlbauer, 1969; Chen, 1992).

In their study on the lyotropic liquid crystal formation of four-stranded aggregates of oligodeoxyguanylates, Bonazzi et al. (1991) measured concentration-dependent CD of d(GpG). The spectrum at the maximum concentration compatible with the isotropic solution exhibits a positive double-humped feature, which upon comparison with that of the four-stranded helix of poly(G) or poly(dG), led them to conclude that the d(GpG) aggregates exhibit the right-handed chirality. Except for the much enhanced intensities, CD spectra exhibited by our $d(TGG)_4$ aggregates are very similar. Thus it is reasonable to infer that the superhelical chirality in our system is also right-handed. This inference is consistent with the mostly positive ψ-CD observed in our system, as Maestre and Reich (1980) had established such a sign correlation with the twist sense of the intermolecular organization of the DNA molecules. Our observations of negative ψ-CD tails in some solutions, however, also suggest the existence of more than one chiral structural form in these aggregates and may partly be responsible for the failure to observe large ψ-CD formations in some of our earlier solutions under somewhat different conditions.

The important role played by Mg^{2+} in the formation of G-quadruplex polymers has been noted by Protozanova and Macgregor (1996), who recently investigated the self-assembly of $d(A_{15}G_{15})$ on native and denaturing electrophoretic gels. The complexes consist of integer numbers of strands ranging from one to more than nine monomers. The relative concentration of the various complexes is determined by the solvent conditions. The complexes are quite stable and are resistant to standard denaturation conditions. Mg^{2+} at fairly low concentration leads to the formation of polymers, whereas the presence of the monovalent cations stabilizes lower-molecular-weight complexes consisting of two to six strands of $d(A_{15}G_{15})$. A model of higher order complexes formed by this oligomer consists of two distinct structural regions, a stem made up of G-tetrads and single-stranded adenosine arms projecting radially from the stem. These polymers are termed "frayed wires," in contrast to the G-wires described by Marsh and Henderson (1994).

To gain further insight into the self-assembly processes of XGG trinucleotide repeats, systematic studies on $d(CGG)_n$, $d(TGG)_n$, $d(AGG)_n$, and some related oligomers are currently being carried out in our laboratory under various solution conditions. It should be noted in passing that our rudimentary measurements indicate that d(GGTGGTGGTGG) exhibits a more facile aggregate-forming ability than $d(TGG)_4$, supporting the crucial role played by terminal guanosines, and $d(TTGG)_4$ failed to exhibit ψ-CD formation or 320-nm absorbance increase in the presence of 2 M KCl and 16 mM Mg^{2+}.

I thank Mary Ann Asson-Batres for her careful reading of the manuscript.

This work was supported by Army Medical Research grant DAMD17-94-J-4474.

REFERENCES

Balagurumoorthy, P., S. K. Brahmachari, D. Mohanty, M. Bansal, and V. Sasisekharan. 1992. Hairpin and parallel quartet structures for telomeric sequences. *Nucleic Acids Res.* 20:4061–4067.

Bonazzi, S., M. Capobianco, M. M. De Morais, A. Garbesi, G. Gottarelli, P. Mariani, M. G. P. Bossi, G. P. Spada, and L. Tondelli. 1991. Four-stranded aggregates of oligodeoxyguanylates forming lyotropic liquid crystals: a study by circular dichroism, optical microscopy, and X-ray diffraction. *J. Am. Chem. Soc.* 113:5809–5816.

Chantot, J. F., and W. Guschlbauer. 1969. Physicochemical properties of nucleosides 3. Gel formation by 8-bromoguanosine. *FEBS Lett.* 4:173–176.

Chen, F.-M. 1992. Sr^{2+} facilitates intermolecular G-quadruplex formation of telomeric sequences. *Biochemistry.* 31:3769–3776.

Chen, F.-M. 1995. Acid-facilitated supramolecular assembly of G-quadruplexes in $d(CGG)_4$. *J. Biol. Chem.* 270:23090–23096.

Dai, T.-Y., S. P. Marotta, and R. D. Sheardy. 1995. Self-assembly of DNA oligomers into high molecular weight species. *Biochemistry.* 34: 3655–3662.

Fasman, G. D., editor. 1975. CRC Handbook of Biochemistry and Molecular Biology, Vol. I, 3rd Ed. CRC Press, Boca Raton, FL. 589.

Fry, M., and L. A. Loeb. 1994. The fragile X syndrome $d(CGG)_n$ nucleotide repeats form a stable tetrahelical structure. *Proc. Natl. Acad. Sci. USA.* 91:4950–4954.

Guo, Q., M. Lu, and N. R. Kallenbach. 1993. Effect of thymine tract length on the structure and stability of model telomeric sequences. *Biochemistry.* 32:3596–3603.

Hardin, C. C., M. Corregan, B. A. Brown, II, and L. N. Frederick. 1993. Cytosine-cytosine$^+$ base pairing stabilizes DNA quadruplexes and cytosine methylation greatly enhances the effect. *Biochemistry.* 32: 5870–5880.

Hardin, C. C., E. Henderson, T. Watson, and J. K. Prosser. 1991. Monovalent cation induced structural transitions in telomeric DNAs: G-DNA folding intermediates. *Biochemistry.* 30:4460–4472.

Hardin, C. C., T. Watson, M. Corregan, and C. Bailey. 1992. Cation-dependent transition between the quadruplex and Watson-Crick hairpin form of $d(CGCG_3GCG)$. *Biochemistry.* 31:833–841.

Lee, J. S. 1990. The stability of polypurine tetraplexes in the presence of mono- and divalent cations. *Nucleic Acids Res.* 18:6057–6060.

Lu, M., Q. Guo, and N. R. Kallenbach. 1992. Structure and stability of sodium and potassium complexes of dT_4G_4 and dT_4G_4T. *Biochemistry.* 31:2455–2459.

Maestre, M. F., and C. Reich. 1980. Contribution of light scattering to the circular dichroism of deoxyribonucleic acid films, deoxyribonucleic acid-polylysine complexes, and deoxyribonucleic acid particles in ethanolic buffers. *Biochemistry.* 19:5214–5223.

Marotta, S. P., P. A. Tamburri, and R. D. Sheardy. 1996. Sequence and environmental effects on the self-assembly of DNA oligomers possessing $G_xT_2G_y$ segments. *Biochemistry.* 35:10484–10492.

Marsh, T. C., and E. Henderson. 1994. G-wires: self-assembly of a telomeric oligonucleotide, d(GGGGTTGGGG), into large superstructures. *Biochemistry.* 33:10718–10724.

Marsh, T. C., J. Vesenka, and E. Henderson. 1995. A new DNA nanostructure, the G-wire, imaged by scanning probe microscopy. *Nucleic Acids Res.* 23:696–700.

Miura, T., J. M. Benevides, and G. J. Thomas, Jr. 1995. A phase diagram for sodium and potassium ion control of polymorphism in telomeric DNA. *J. Mol. Biol.* 234:1171–1183.

Protozanova, E., and R. B. Macgregor, Jr. 1996. Frayed wires: a thermally stable form of DNA with two distinct structural domains. *Biochemistry.* 35:16638–16645.

Reich, C., M. F. Maestre, S. Edmondson, and D. M. Gray. 1980. Circular dichroism and fluorescence-detected circular dichroism of deoxyribonucleic acid and poly[d(A-C)·d(G-T)] in ethanolic solutions: a new method for estimating circular intensity differential scattering. *Biochemistry.* 19:5208–5213.

Rippe, K., V. Fritsch, E. Westhof, and T. M. Jovin. 1992. Parallel-stranded DNA, potential intervention of a stable double-helical structure in recombination. *EMBO J.* 11:3777–3786.

Sen, D., and W. Gilbert. 1992. Novel DNA superstructures formed by telomere-like oligomers. *Biochemistry.* 31:65–70.

Shin, Y. A., and G. L. Eichhorn. 1984. Formation of $\psi(+)$ and $\psi(-)$ DNA. *Biopolymers.* 23:325–335.

Suda, T., Y. Mishima, H. Asakura, and R. Kominami. 1995. Formation of a parallel-stranded DNA homoduplex by d(GGA) repeat oligonucleotides. *Nucleic Acids Res.* 23:3771–3777.